

TITLE PAGE

Clinical, imaging genetics and deformation based morphometry study of longitudinal changes after surgery for intractable aggressive behaviour

Authors: Flavia V. Gouveia^{1,2*}, Jürgen Germann^{3*}, Rosa M. C. B. de Morais⁴, Erich T. Fonoff⁵,
5 Clement Hamani^{2,5,6}, Eduardo Joaquim Alho⁵, Helena Brentani^{7,8}, Ana Paula Martins⁴, Gabriel Devenyi³, Raihaan Patel³, Christopher J. Steele³, Robert Gramer⁹, M. Mallar Chakravarty³, Raquel C. R. Martinez^{1†}.

1. Laboratory of Neuromodulation, Teaching and Research Institute, Hospital Sírio-Libanês, São Paulo, São Paulo, Brazil.
- 10 2. Neuromodulation Centre, Sunnybrook Research Institute, University of Toronto, Toronto, Ontario, Canada.
3. CIC, Douglas Mental Health University Institute, McGill University, Montreal, Quebec, Canada
4. PROTEA, Department of Psychiatry - University of São Paulo School of Medicine, São Paulo, São Paulo, Brazil.
- 15 5. Department of Neurology, Division of Functional Neurosurgery of the Institute of Psychiatry, University of São Paulo, Medical School, São Paulo, São Paulo, Brazil.
6. Division of Neurosurgery, Sunnybrook Health Sciences Centre, University of Toronto, Toronto, Ontario, Canada
7. Department of Psychiatry - University of São Paulo, Medical School, São Paulo, São Paulo, Brazil.
- 20 8. National Institute of Developmental Psychiatry for Children and Adolescents, CNPq, São Paulo, São Paulo, Brazil.
9. Department of Neurosurgery, Duke University Medical Center, Durham, North Carolina, United States

*These authors have contributed equally to this work.

25 **†Corresponding Author:**

Raquel Chacon Ruiz Martinez, Ph.D.
Instituto de Ensino e Pesquisa - Hospital Sírio Libanês
Rua Professor Daher Cutait, 69
Zip Code: 01308-060 - São Paulo - SP - Brazil
30 Phone: +551133944779; Fax: +551131554220
Email: quelmartinez@yahoo.com.br

ABSTRACT

Intractable aggressive behaviour is a devastating behavioural disorder that reach 30% of psychiatric aggressive patients. Neuromodulatory surgeries may be treatment alternatives to reduce suffering. We investigated the outcomes of bilateral amygdala radiofrequency ablation in four patients with intractable aggressive behaviour (life-threatening-self-injury and social aggression) by studying whole brain magnetic resonance imaging and clinical data. Post-surgery assessments revealed decreases in aggression and agitation and improvements in quality of life. Aggressive behaviour was positively correlated with serum testosterone levels and the testosterone/cortisol ratio in males. No clinically significant side effects were observed. Imaging analyses revealed preoperative amygdala volumes within normal range and confirmed appropriate lesion locations. Reduction in aggressiveness were accompanied by volumetric reduction in brain areas associated with aggressive behaviour (express genes related to aggressive behaviour), and increases in regions related to somatosensation. These findings further elucidates the neurocircuitry of aggression and suggests novel neuromodulation targets.

Keywords: Aggressive Behavior; Amygdala; Testosterone; Magnetic Ressonance Imaging; Deformation Based Morphometry; Neurosurgery.

INTRODUCTION

Excessive aggressive behavior is highly prevalent in patients with Autism Spectrum
50 Disorder (ASD) and Intellectual Disabilities (ID)¹. It presents a major obstacle to patient care and treatment². Additionally, it often presents as severe self-injurious behavior that may culminate with the need for chronic restraining of patients, substantially reducing quality of life^{3,4}. The primary treatment for excessive aggressive behavior involves the use of behavioral therapy and medications that act mainly on dopaminergic and serotonergic systems^{1,5}. When patients fail to respond to
55 conventional behavioral and medical treatments, high dose mono- or polypharmacy strategies are indicated⁶. Although these therapies are successful in most patients, there is a significant subset of individuals (approximately 30%) who do not adequately respond to treatment and are considered medication-refractory⁷.

Structures related to the control of aggressive behavior include the prefrontal cortex,
60 amygdala, hypothalamus and midbrain periaqueductal gray⁸. It is believed that aggressive individuals have alterations in these structures. Prior research suggests that higher limbic system activity alters perception of provocative stimuli, and reduces “top-down” control of the prefrontal cortex, minimizing the ability to suppress aggressive behavior⁸. Lesion studies performed in the late 18th and early 19th centuries have shown that the removal of the temporal lobes or selective
65 amygdala ablation resulted in marked reduction of aggressive behavior in humans⁹⁻¹¹ and nonhuman primates^{12,13}. Imaging studies have been largely controversial and/or inconclusive in asserting an association between amygdala volume¹⁴ or activity¹⁵ and behavioral disorders (including aggressive behavior). For example, veterans with aggressive behavior disorders have been shown to demonstrate a more intense amygdala response to external stimuli as well as an attenuated
70 amygdala-prefrontal cortex connectivity^{15,16}. In contrast, studies in criminal psychopaths have

reported that the level of amygdala activation is lower during processing of negative affective stimuli, fear conditioning paradigms, and emotional moral decision making^{17,18}.

More recently, amygdala deep brain stimulation (DBS) was successfully used to reduce aggressive behavior (life-threatening self-injurious behavior) in a drug-refractory autistic teenager³.

75 Quite often, however, patients with severe self-aggressive behavior towards the face and head are precluded from DBS consideration for fear of complications such as infection, skin erosion, and lead fracture¹⁹. For this small population of non-responsive individuals, stereotactic ablative surgery targeting the amygdala has been performed with beneficial result^{11,20}. As this patient population is small and the number of recent publications are limited, in depth clinical follow up and the study of
80 neuroanatomical and/or functional aspects of this surgery remain sparse. In particular, to date, no study has attempted to identify and characterize the brain morphology and changes associated with surgical intervention in these subjects.

We addressed the crucial gap in understanding the aggressive brain circuitry and how structural and functional changes in this network relate to behavior changes by studying
85 longitudinal local volume and structure changes throughout the whole brain and examining the clinical and hormonal effects of bilateral amygdala radiofrequency ablation in a small cohort of patients with aggressive behavior.

RESULTS

Behavior assessments demonstrated a marked reduction in aggressive behavior in all
90 patients (p01: 84.6%; p02: 80%; p03: 88.9%; p04: 56.2%; p_(cor)<0.01; Figure 1E). This was associated with a reduction in motor agitation (p_(cor)<0.05; Figure 1F) and an increase in quality of life (p_(cor)<0.01; Figure 1G). Significant correlations were found between improvements in aggressive behavior and agitation (p<0.0001) and between improvements in aggressive behavior and quality of life (p=0.01612; Supplementary Figures 1A-B).

95 Each total amygdala volume was measured before the surgical procedure and was determined to be within normal range²¹ (Figure 1A-D). After surgery, we confirmed the location of the lesion and measured its size. As shown in Figure 1D, lesions were smaller in volume than the amygdala. P01, p02 and p04 required a second procedure, after which most of the amygdala was ablated.

100 The ratio between testosterone and cortisol is a biomarker for aggressive behavior²². We identified a positive correlation between aggressive behavior and the testosterone/cortisol ratio in the males ($p_{(cor)}<0.01$, Figure 1H; p01 $p=0.0205$; p02 $p=0.0243$; p03 $p=0.0334$; p04 $p=0.315$; Supplementary Figures 1D-G) and between aggressive behavior and total testosterone, also only in the male patients ($p=0.00101$; p01 $p=0.0142$; p02 $p=0.0584$; p03 $p=0.0247$; p04 $p=0.8059$,
105 Supplementary Figures 1C and 2H-K). Although some fluctuation in the hormone levels occurred, there was no significant clinical impact on patients well-being (Supplementary Table 1).

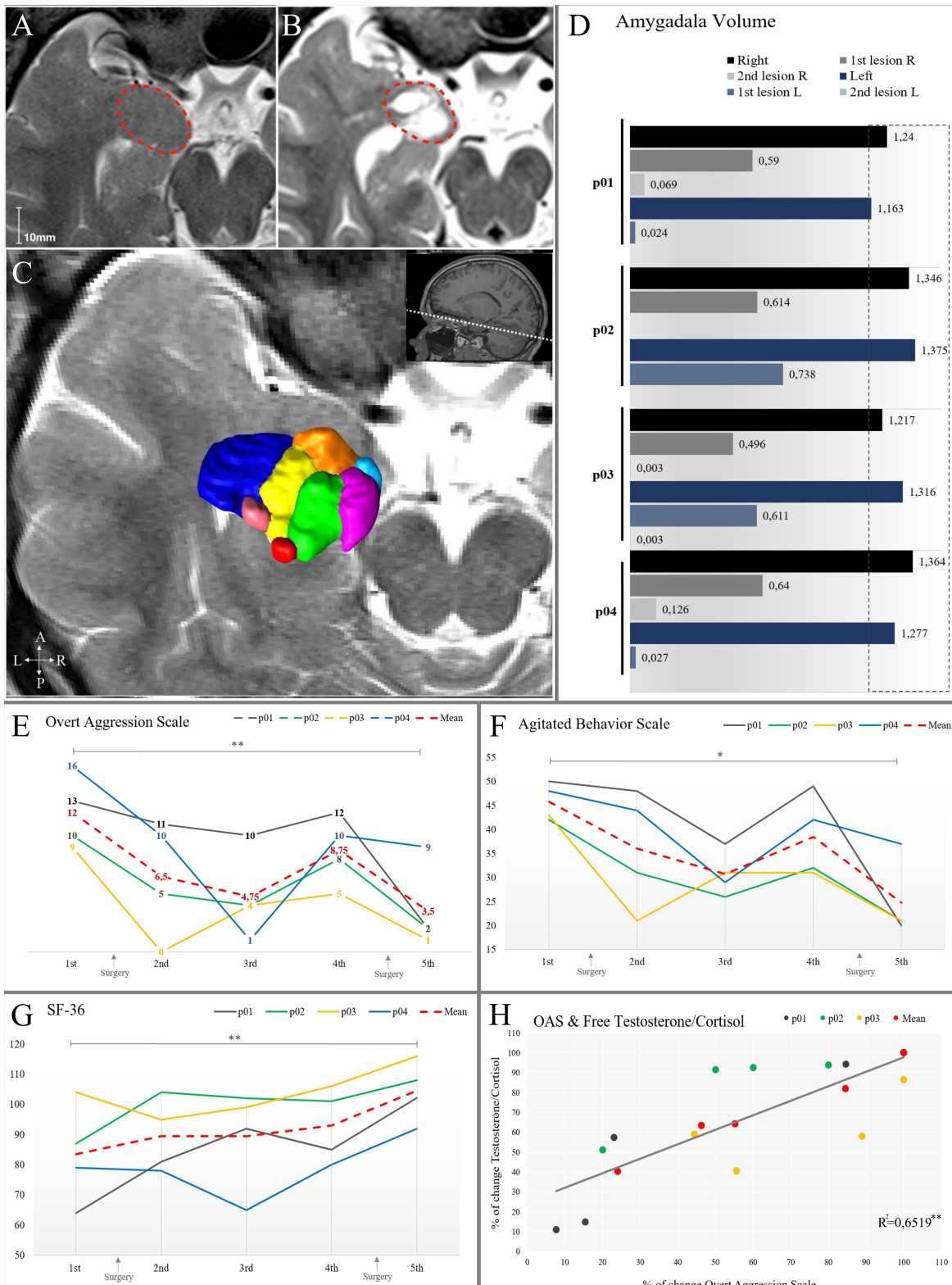


Figure 1. Baseline and follow up evaluations. A. MRI image showing amygdala location before surgery. B. MRI image showing lesion placement. C. 3D reconstruction of the amygdala on an MRI image. D. Amygdala volume; E. Aggressive levels measured by the Overt Aggression Scale (OAS); F. General motor agitation measured by the Agitated Behavior Scale (ABS); G. Quality of life evaluated by the Short Form Survey (SF-36); H: Correlation between the testosterone/cortisol ratio and aggressive behavior for male patients (p01, p02, p03, mean). Abbreviations: 1st: Baseline evaluation; 2nd: 3 months after surgery; 3rd: 12 months after surgery; 4th: 24 months after surgery; 5th: 36 months after surgery for p03 and after 2nd surgery for p01, p02 and p04. * $p<0,05$, ** $p<0,01$.

The longitudinal DBM analysis of these patients (Figure 2) identified significant morphological changes in several brain regions. Volumetric decrease was found in many areas, 115 including those known to play a role in mechanisms of aggressive behavior (e.g. doroslateral prefrontal cortex (DLPFC), nucleus accumbens (NAcc), bed nucleus of stria terminalis (BNST))^{8,23}. Volume increases were observed in areas involved in somatosensory processing and pain perception (e.g. somatosensory cortex, thalamus)²⁴. Supplementary Figure 2 illustrates the volume change in those and other main regions. Table 1 lists and names the key peaks passing FDR correction 120 ($q < 0.01$) their t-value and FA and MD percent change.

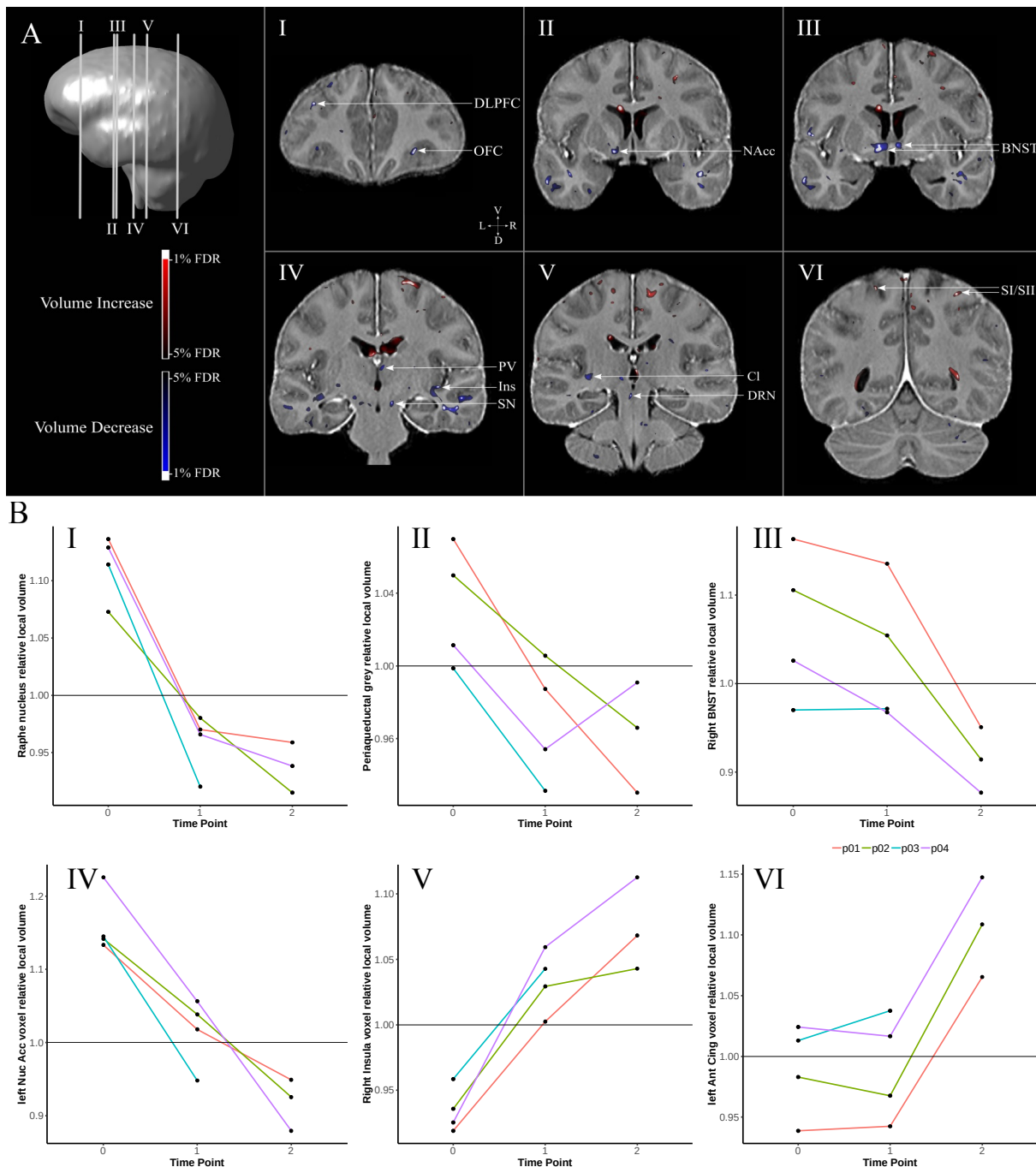


Figure 2. Results from Deformation Based Morphometry analysis (DBM). A. Coronal slices illustrating areas that presented significant local volume changes in the longitudinal DBM analysis. The areas named are known to be part of the neurocircuitry of aggressive behavior or somatosensation. B. Changes overtime in selected peak voxels in each patient. Data is presented as scale of relative voxel size. I. Dorsal Raphe nucleus; II. Periaqueductal Gray; III. Right Bed Nucleus of Stria Terminalis; IV. Left Nucleus Accumbens; V. Right Insula; VI. Left Anterior Cingulate. Abbreviations: BNST: bed nucleus of stria terminalis; Cl: claustrum; ex: cortex; DLPFC: dorsolateral prefrontal cortex; DRN: dorsal raphe nucleus; Ins: insula; int: internal; L: left; lam: lamina; NAcc: nucleus accumbens; nu: nucleus; OFC: orbitofrontal cortex; PV: paraventricular thalamic nucleus; R:right; SI/SII: somatosensory cortex; SN: substantia nigra.

Table 1. Longitudinal analysis with DBM and FA/MD maps

Anatomical Structure	MNI space coordinates			JD	% change	
	x	y	z		t value	FA
L inferior longitudinal fasciculus	-43.87	-23.68	-15.24	-50.98**	7.465	8.596
R inferior longitudinal fasciculus	48.32	-27.76	-17.15	-44.03**	-1.114	8.607
L orbitofrontal cortex	-9.43	47.56	-22.36	-34.87**	6.544	8.361
L raphe nucleus	-1.14	-29.83	-11.95	-33.97**	-2.09	15.191
R periaqueductal gray	2.19	-32.83	-9.29	-31.06**	-25.572	9.216
R bed nucleus of stria terminalis	3.10	2.43	-3.69	-28.96**	-19.958	6.923
R paraventricular thalamic nucleus	1.85	-11.11	8.10	-24.14**	-26.399	37.175
R substantia nigra	9.11	-19.10	-15.35	-23.85**	-4.049	2.63
L dorsolateral prefrontal cortex	-31.37	49.28	18.17	-23.06**	-1.682	41.129
L substantia nigra	-10.54	-18.28	-13.90	-23.06**	-9.62	9.388
R medial dorsal thalamic nucleus	3.05	-11.18	8.74	-22.21**	-32.317	16.894
R orbitofrontal cortex	25.53	36.57	-13.69	-20.65**	-3.071	10.494
R claustrum	29.87	14.09	3.41	-20.24**	-5.101	7.922
R ventral lateral thalamic nucleus	18.99	-13.32	9.64	-19.78**	-5.216	-0.081
R inferior semilunar lobule	10.88	-80.50	-33.16	-18.72**	-14.3	9.629
L dentate nucleus	-22.59	-52.86	-36.89	-18.51**	-4.416	7.262
R pulvinar thalamic nucleus	11.64	-22.98	12.12	-18.26**	-30.583	4.521
R dentate nucleus	19.13	-49.84	-37.45	-18.26**	-14.292	28.316
L insula	-38.88	1.90	10.07	-18.01**	4.784	26.966
R accumbens	9.43	6.31	-11.97	-17.5**	2.274	17.973
L frontoparietal operculum	-51.99	0.81	4.50	-17.13**	16.576	-5.362
R dorsolateral prefrontal cortex	34.22	49.34	22.33	-15.28**	-3.081	5.113
L inferior semilunar lobule	-20.15	-82.17	-33.10	-14.36**	-14.524	11.664
L red nucleus	-6.38	-24.51	-15.23	-13.21**	-8.359	5.776
R internal medullary lamina of thalamus	8.92	-7.53	4.90	-13.03**	-8.846	3.332
R red nucleus	5.85	-25.63	-15.23	-13.03**	-3.829	-2.177
R insula	40.34	-15.42	-3.35	-12.54**	16.973	10.083
L accumbens	-12.49	5.25	-10.24	-11.68**	2.754	14.47
L bed nucleus of stria terminalis	-7.93	2.97	-4.98	-11.68**	0.314	21.048
R frontoparietal operculum	44.76	-3.38	14.60	-11.26**	3.385	-4.442
R corpus callosum	5.94	22.48	11.50	11.91**	3.775	6.887
L frontopolar cortex	-25.77	66.70	2.89	12.45**	-20.777	-1.377
L insula	-38.44	19.97	2.23	12.54**	0.499	1.47
R parafascicular thalamic nucleus	7.63	-17.92	-1.54	12.59**	-7.486	-8.679
L somatosensory cortex	-14.93	-32.32	73.56	13.37**	21.858	-11.233
R insula	35.76	-19.48	6.69	13.43**	-1.661	-5.895
R hippocampus	34.31	-31.37	-6.28	13.47**	-2.754	8.951
R frontopolar cortex	17.78	68.63	10.21	14.74**	-10.237	-0.271
R somatosensory cortex	39.19	-35.29	71.31	20.84**	-12.002	-9.483
L anterior cingulate gyrus	-6.36	34.98	28.74	23.59**	-10.04	10.729
R anterior cingulate gyrus	3.21	31.04	27.07	28.37**	7.229	3.567

L corpus callosum -7.47 17.28 17.06 48.3** 13.996 -5.783

Abbreviations: L: left; R: Right; JD: Jacobian Determinant, from DBM analysis; FA: Fractional Anisotropy; MD: Mean Diffusivity. All peaks pass voxel level FDR whole brain correction for multiple correction with ** $q < 0.01$ (absolute t-value > 10.7). Thus at the most there is one false positive finding per 100 significant peak voxels. Local changes at the voxel level are calculated within subject and co-registered for subsequent group level analysis. MNI space (MNI icbm152 nlin sym09c).

Likewise, both FA and MD changed after surgery and there was a significant correlation between changes in Jacobians and MD, which is related to the displacement of water (FA $p_{(cor)} > 0.05$; MD $p_{(cor)} < 0.05$; Figure 3A for main peaks. Supplementary Figure 3 for all peaks).

Hierarchical clustering was applied to investigate the possibility of groupings within brain areas that were significant in the DBM analysis. The results confirmed the presence of 2 clusters: Cluster 1: areas that decrease in volume known to be related to aggressive behavior and connected to the amygdala^{8,23}; Cluster 2: areas that increase in volume involved in somatosensation and pain perception²⁴ (Figure 3B).

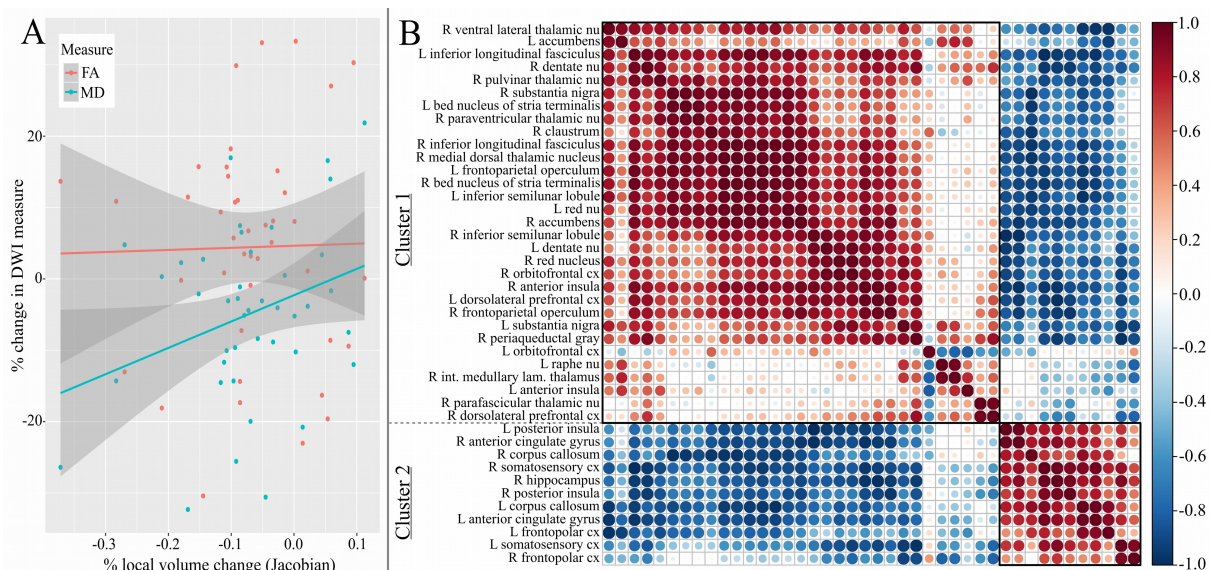
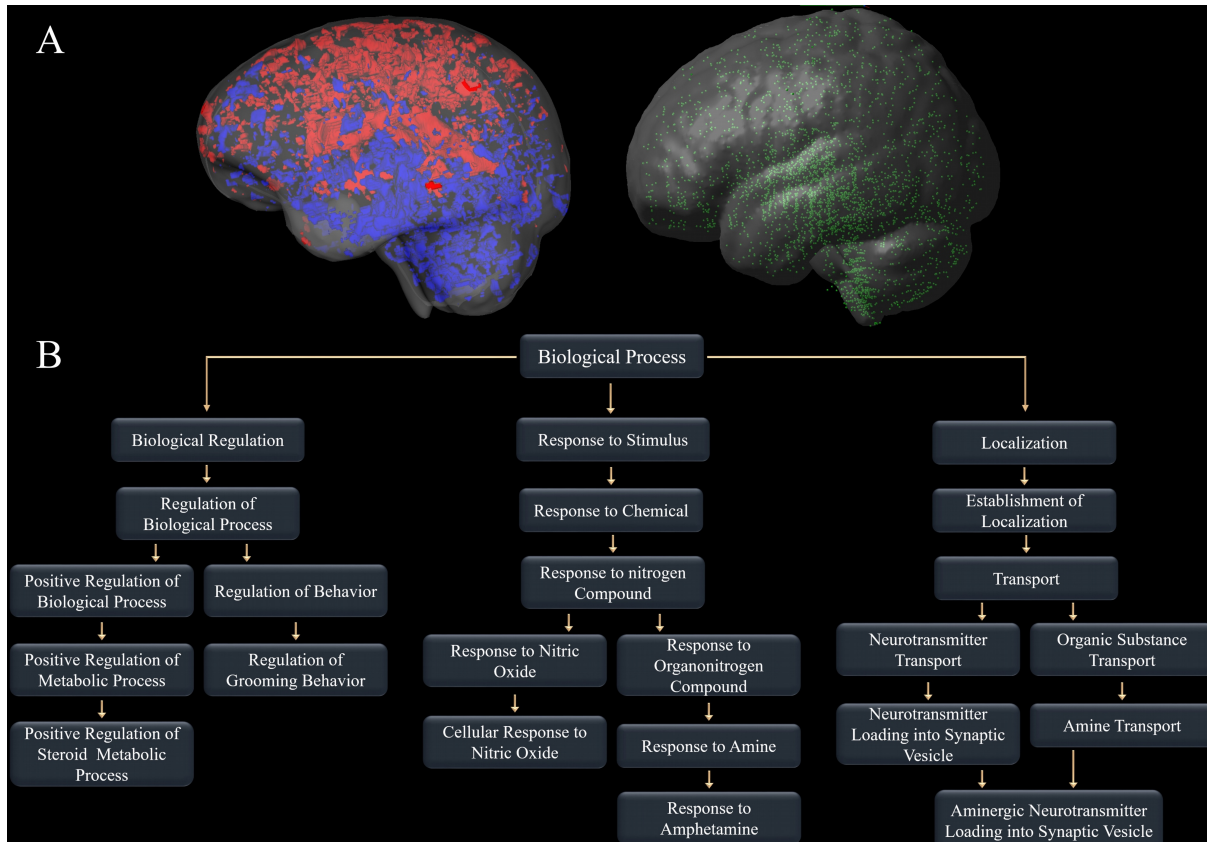


Figure 3. Results from Fractional Anisotropy (FA) and Mean Diffusivity (MD) maps and Cluster analysis of the Deformation Based Morphometry study. A. Correlation between DBM Jacobians, FA and MD maps for main peaks. B. Hierarchical cluster of DBM peaks (5% FDR correction).

The gene ontology analysis of the genes highly expressed in regions that exhibited morphological shrinkage (Cluster 1) compared to the rest of the brain showed functions related to amygdala and aggressive behavior: 1. Steroid metabolic process; 2. Regulation of grooming behavior; 3. Response to chemicals Nitric oxide and Amphetamine; 4. Aminergic neurotransmitter

transport. Figure 4 shows these results and the complete gene enrichment analysis can be found in Supplementary Figure 4.



135 **Figure 4.** Results of gene enrichment analysis. A. Illustration of the inside/area genetic enrichment analysis. The left side shows the distribution of DBM results (10% FDR corrected) red represents increases and blue decreases in volume. The right shows the location where tissue samples were collected for the gene expression analysis. Every green dot indicates a well location. B. Summary of GOrilla and GEAS gene enrichment analysis results for decreased Jacobians and overexpressed genes.

DISCUSSION

140 Stereotactic surgery led to a remarkable reduction in aggressive behavior and improvements in quality of life in patients with medically-refractory aggressive behavior. To assess potential therapeutic mechanisms for the procedure, MRI images acquired before and after the surgery were analyzed using DBM, and FA and MD maps computed. While the DBM technique uses image registration to calculate local deformation fields at a voxel level for the detection of morphological variations²⁵, FA and MD values are indicative of local microstructural characteristics primarily related to white matter. FA is an index of diffusion asymmetry and is related to characteristics such

as fiber density, axonal diameter and myelination, while MD shows the degree of displacement of water molecules²⁶.

We found that morphological changes associated with reduction in aggressive behavior
150 could be grouped into two clusters: Cluster 1 includes areas associated with aggressive behavior such as the DLPFC, NAcc, BNST, Insula, periaqueductal gray (PAG), and dorsal raphe nucleus (DRN). Cluster 2 regions includes areas related to somatosensation and pain perception, such as somatosensory cortex, thalamus, and anterior Cingulate Cortex. The correlation of volumetric changes with DWI measures suggests that the volume change following surgery is related to local
155 microstructural changes. Though the exact mechanism driving these distinct changes remains unexplained (e.g. increase/decrease of number of glial cells, hypo- or hypertrophy of neurons), it is interesting to note the clusters change in opposite directions. Areas of cluster 1 receive alert signals from the presumably hyperactive amygdala⁸ and decrease in volume once the amygdala stimulation ceases. Whereas, activity in the regions of cluster 2 are suppressed when the amygdala is highly
160 activated and increase in volume post-surgery. The distinct pattern of local changes throughout the somatosensory/pain network is particularly intriguing in this group and may explain the reduction in self-aggressive behavior observed after surgery (OAS self-injury subscale change: p01: 4 to 1; p02: 1 to 0; p03: 4 to 0; p04: 4 to 2). It is known that the amygdala has a central role in processing nociceptive²⁷ stimuli and that patients with self-injurious behavior have altered pain perception²⁸.
165 Thus, amygdala ablation could affect this neurocircuitry, restoring normal activity in areas related to the process of nociceptive stimuli resulting in reduction of self-injury behavior.

The correlation found between aggressive behavior and agitation supports the theory that excessive aggressive behavior occurs when the amygdala is hyper-activated and more responsive to environmental stimuli⁸. In fact, after surgery, patients were able to return to a special needs school
170 that they were previously forced to withdraw from when their condition had progressively worsened. There they are able to learn and improve skills, mainly related to daily life activity

and communication. In this sense, the procedure appears to leads to significant behavioral improvement which enables patients to function in a social construct that fosters further behavioral improvement. Although permanent side effects and worsened behavioral problems have been
175 previously reported^{9,11,19}, an important aspect of our study was that no noticeable side effects were observed after surgery.

The gene ontology analysis found that Cluster 1 regions are related to steroid metabolic process, response to Nitric oxide and Amphetamine, aminergic neurotransmitter transport, and interestingly, regulation of grooming behavior. These all are closely related to the amygdala and
180 aggressive behavior: Grooming behavior is similar to aggressive behaviors in the sense that it is an innate social behavior influenced by the amygdala, which plays an important role in social bonding and the maintenance of species²⁹. The aminergic neurotransmitter system (e.g. serotonin and dopamine) as well as nitric oxide and amphetamine have all been implicated in the modulation of aggressive behavio^{5,30,31}. The mechanism for this effect, however, is still unknown. Steroid
185 metabolism is a process linked to aggressive behavior and is influenced by the amygdala via extensive bi-directional projections to and from the hypothalamus. This latter structure is responsible for controlling hormonal production and secretion including precursors of the synthesis of testosterone and cortisol³². These two hormones are part of internal feedback loops of the amygdala resulting in the expression of more aggressive actions (consequence of testosterone
190 augmentation) or increased fear responses (consequence of cortisol predominance). It is believed that the ratio between those two hormones may be a biomarker for aggressive behavior²². In fact, this is reinforced by the correlation found between testosterone and the testosterone/cortisol ratio and aggression.

To our knowledge, this is the first report of longitudinal neuroimaging analyses of patients
195 treated with bilateral amygdala radiofrequency ablation. DBM analyses enabled the detection of subtle local volumetric changes throughout the brain and helped us identify numerous local

structural alterations that accompany the behavioral changes. We observed consistent characteristic changes within our patients and we believe that this analysis better elucidates the whole human neurocircuitry of aggressive behavior and provides new insights for future interventions. All the
200 changes result in striking behavior alterations leading to easing of suffering and improvement in quality of life. The changes essential and necessary for the positive outcome are yet to be elucidated. Expounding these connections through future research could be instrumental in deriving a better understanding this complex neurocircuitry as well as its mechanism in modulating behavior. Our results, however, suggest an interesting starting point to investigate possible new targets for
205 intervention. For example, one could propose the use of non-invasive neuromodulatory techniques (e.g. Transcranial Magnetic Stimulation (TMS), Transcranial direct current stimulation (tDCS)) delivered to somatosensory cortical areas or DBS to the NAcc or BNST, for the treatment of patients with excessive aggressive behavior. Furthermore, these results highlight the need for studies to ascertain the cause of morphological changes, identify the population of neurons being
210 affected, and explore the impact of these changes on neurotransmitter systems, especially in the context of the aminergic system.

In summary, our results provide novel evidence that bilateral amygdala ablation induces re-adaptation of the neurocircuitry that controls aggressive behavior, with a concomitant behavioral phenotype. These morphological changes could be integral to the reduction of aggressive behavior
215 and increase in quality of life observed in our study population. Further research is necessary to better understand this complex neurocircuitry and explore new targets for therapeutic interventions and less invasive techniques.

METHODS AND MATERIALS

SUBJECTS

220 Four patients with intractable aggressive behavior (3 males, 1 female; aged 19-32 years; demographics in Table 2) were included in the study following psychiatric referral from our outpatient psychiatric clinic. All subjects were diagnosed with severe ID and the 3 males also with ASD. All patients showed uncontrollable life-threatening-self-injurious behavior and extreme aggressive behavior towards their surroundings and others. Three patients required restraint
225 measures on a daily basis. The subjects were selected for the ablation procedure as their severe self-aggressive behavior made them non-eligible for DBS¹⁹. An experienced multidisciplinary team assisted the patients and caregivers at all times. Patients' psychiatric histories are presented in Supplementary Text 1. Criteria for patient selection and for defining treatment refractoriness followed the mandate for conducting psychiatric surgery stipulated by the Regional and Federal
230 Medical Councils. All study procedures, logs, and results were documented and archived in accordance with the Research Ethical Board (#CAPPesq742.331; #CAAE31828014.6.3001.5461). The patient's parents provided written informed consent after being instructed about potential risks and benefits of surgical treatment. The study was registered as a clinical trial at <https://clinicaltrials.gov> (#NCT03452878).

Table 2. Demographics and clinical characteristics

Patient	Karyotype	Main diagnosis	Intellectual capacity	Preoperative medication
p01	46,XY normal	Autism spectrum disorder	Severely impaired	Aripiprazole; Biperiden; Carbamazepine; Chlorpromazine; Clozapine; Divalproex sodium; Haloperidol; Levomepromazine; Olanzapine; Promethazine; Quetiapine fumarate; Risperidone; Thioridazine; Ziprasidone
p02	46,XY normal	Autism spectrum disorder	Severely impaired	Aripiprazole; Benzodiazepines; Biperiden; Carbamazepine; Chlorpromazine; Clonidine; Clozapine; Divalproex sodium; Haloperidol; Levomepromazine; Olanzapine; Promethazine; Risperidone; Thioridazine; Topiramate

p03	46,XY normal	Autism spectrum disorder	Severely impaired	Aripiprazole; Biperiden; Carbamazepine; Chlorpromazine; Clomipramine; Divalproex sodium; Haloperidol; Levomepromazine; Olanzapine; Oxcarbazepine; Promethazine; Quetiapine fumarate; Risperidone; Sertraline; Thioridazine; Topiramate; Ziprasidone
p04	46,XX normal	Intellectual disabilities	Severely impaired	Aripiprazole; Carbamazepine; Chlorpromazine; Divalproex sodium; Fluoxetine; Haloperidol; Levomepromazine; Lithium; Methylphenidate; Mirtazapine; Olanzapine; Quetiapine fumarate; Risperidone; Topiramate

235 PRE AND POSTOPERATIVE EVALUATIONS

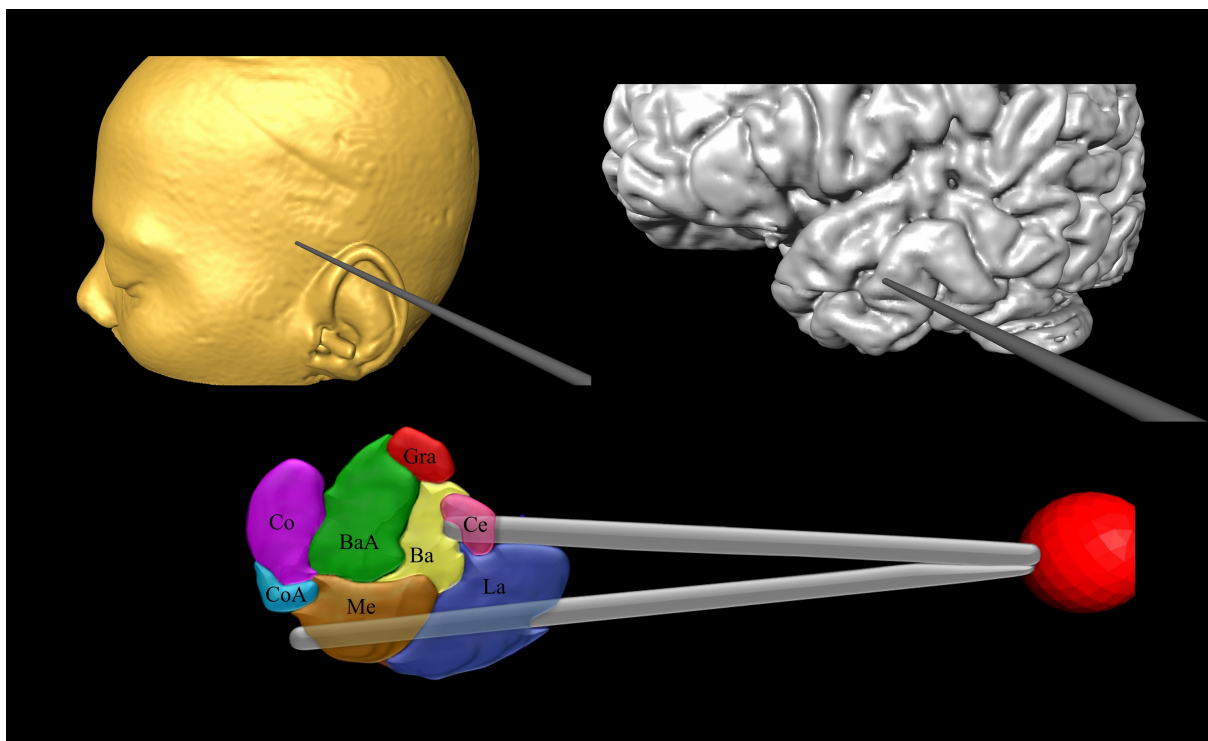
Preoperative assessment involved full clinical, psychiatric, and neurosurgical evaluations as well as whole brain magnetic resonance imaging (MRI). Questionnaires quantified aggressive behavior, general motor agitation, and quality of life with the Overt Aggression Scale (OAS), Agitated Behavior Scale (ABS), and Short Form Survey (SF-36), respectively. Laboratory tests 240 included: thyroid, kidney, and liver function, adrenal and gonadal hormone levels; lipid, coagulation, and inflammation profiles; and complete blood count (Supplementary Table 1). Since patients presented with severe intellectual disability, neuropsychological evaluations were deferred.

Postoperative follow up included all preoperative measures and was performed at 3, 12, 24 and 36 months after surgery. Patients p01, p02 and p04 needed a second surgery 24 months after the 245 first to increase lesion size, characterized on imaging as well as by minimal symptomatic benefits. Their follow-up was indexed from the date of the first operation. Supplementary Figure 5 illustrates the study timeline.

SURGERY

The surgeries were completed under local anesthesia and sedation. Following a preoperative 250 MRI, a Leksell stereotactic frame (Elekta AB, Sweden) was applied to the patient's head and a stereotactic computed tomography was obtained. Imaging data was transferred to the iPlan®

Stereotaxy software (Brainlab - Feldkirchen, Germany) for calculation of optimal tridimensional coordinates for the inferior and superior aspects of the proposed lesion, as well as for the entry point and trajectory of the radiofrequency probe. A two millimeter straight probe was introduced through a
255 twist drill burr hole in the coordinates of the inferior aspect of the lesion, medial part. A radio frequency lesion was then applied at 80°C for 90 seconds. The probe was adjusted three millimeters laterally, and a second lesion was placed, followed by a third and fourth lesion at the superior coordinates. This procedure was repeated for the contralateral amygdala. Figure 5 illustrates probe placement.



260 **Figure 5.** 3D reconstructions of probe placement in the amygdala. Abbreviations: Ba: Basalis; BaA: Basalis accessorius; Ce: Centralis; Co: Corticalis; CaA: Corticalis accessorius; Gra: Granularis; La: Lateralis; Me: Medialis.

MRI AQUISITION

Scans were obtained on a 1.5 Tesla MRI system (Magnetom Espree, Siemens, Germany).
T1-weighted structural images (slice thickness 1.0 mm, no gap, TE/TR 5/300 ms, flip angle 45°,
265 FOV 240 mm, 1 x 0.9 x 0.9 mm or 1 x 0.5 x 0.5 mm voxel) and diffusion-weighted images (DWI)
(4.0 mm slice thickness, gap 0.5 mm, TE/TR 5000/100 ms, flip angle 45°, FOV 240 mm, 4 x 2 x 2

mm voxel, b=1000, 36 directions, 3 b0 images) were acquired. Images were resampled to 0.5mm isotropic voxels for Deformation Based Morphometry (DBM) analysis. The Fractional Anisotropy (FA) and Mean Diffusivity (MD) maps were computed at native resolution and then coregistered
270 with the resampled T1-weighted images resulting from the DBM analysis.

IMAGE PROCESSING

Presurgical amygdala volume and post-surgical lesion size were estimated using Amira® 3D (FEI Houston Company, USA). For the remaining analysis, amygdala lesion and area of the probe entry were excluded. T1-weighted images were non-uniformity corrected and skull-stripped³³. To
275 capture changes in local brain morphology, we used DBM, a technique based on image registration. Image registration produces transformations that map every point in one image to its corresponding point in another image. Thus, it allows for detection and quantification of anatomic differences. In this sense, longitudinal changes were evaluated by DBM using the ANTs toolkit (<http://stnava.github.io/ANTs/>; ‘antsMultivariateTemplateConstruction2.sh’)³³ for linear and non-
280 linear registration in a 2 level registration procedure where we first registered all images of the same subject to one another to detect within subject changes occurring over time – the critical variable of interest for the analysis of the lesion effect.

In a second registration, we registered the subject averages to one another to achieve voxel correspondence to compare the local individual changes across the group of subjects. Local
285 volumetric changes of each voxel within each image are captured in the Jacobian of the deformation from the image registration, and have been shown to be sensitive to anatomical changes within the brain without requiring a priori segmentation²⁵. Especially within-subject longitudinal DBM has been shown to be capable of detecting small local brain changes³⁴. The Jacobians were calculated within each subject, transformed to the group average and smoothed using a 2 mm gaussian 3D
290 kernel.

DWI images were analyzed using the MRtrix package (J-D Tournier, Brain Research Institute, Australia, <https://github.com/MRtrix3/mrtrix3>)³⁵. Raw images were first corrected for distortions and motion³⁶ within each acquisition, and then denoised³⁷ before calculating the diffusion tensor. FA and MD maps were then computed from the diffusion tensor. To achieve local correspondence between the DWI and the DBM measures, the individual DWI images were coregistered with the corresponding individual T1-weighted images and mapped onto the group average of the DBM analysis. FA and MD maps were subsequently blurred using a 2 mm gaussian 3D kernel. Local MD and FA values were extracted in regions that showed significant local volume changes to investigate the possible microstructural changes.

300 STATISTICS

The RMINC (<https://github.com/Mouse-Imaging-Centre/RMINC>) package in RStudio (version 3.3.3, <https://www.r-project.org/>) was used for statistical analysis. A linear mixed-effect model was performed. To test changes over time and the relationship between behavior and hormone evaluation we used a linear mixed effect model with subject as random effect.

305 For imaging analysis, the model tested local change at every voxel over time with the three timepoints as ordered factor as fixed and patient and random effect. T- statistics for linear and quadratic trajectories of change across time were calculated at each voxel and corrected for multiple comparisons using false discovery rate (FDR). The level of significance was set at $q < 0.05$ (whole brain FDR-correction) for all DBM analyses. To investigate possible patterns in the DBM results, a
310 hierarchical clustering analysis was performed. The input was a cross correlation matrix, where element (x,y) describes the correlation of computed Jacobians between region x and region y across all 4 subjects. The agglomerative clustering algorithm from sci-kit learn (<http://scikit-learn.org/>) was used with ward linkage criterion. In this method, each observation (i.e., vector of correlations) starts as its own cluster before clusters are successively merged together based on their similarity.

315 Maps of volumetric change were used to identify regions of interest (ROI) for inside/outside
genetic enrichment analysis of areas that grew or shrunk significantly over time compared to the
rest of the brain using the Allen Institute human gene expression data³⁸ (© 2010 Allen Institute for
Brain Science. Allen Human Brain Atlas. human.brain-map.org). T-stat maps were thresholded at $|t|$
 >2.66 ($q<0.1$ whole brain FDR corrected; this threshold is necessary to get a more expansive spatial
320 map of volumetric changes to colocalize with brain areas included in the Allen brain atlas). The
well locations used for the Allen gene atlas were registered to common space and each well location
was given a spatial extent of a sphere with radius 2mm. T-stat maps were registered to common
space, binarized, and a mixed effects linear model with Age and Sex as fixed effect covariates as
well as Allen subject ID as a random effect covariate were used to compare the genetic expression
325 inside versus outside the binarized map. Inside versus outside gene significance was then adjusted
for multiple comparisons using bonferroni correction ($p_{cor}<0.05$) sorted and split for positive and
negative t-statistics (genes enriched versus underexpressed within versus the rest of the brain).
Finally the ranked gene orders were used as inputs for gene enrichment analysis using the
Gorilla³⁹ and GEAS⁴⁰ tools.

330 **ACKNOWLEDGEMENTS**

The authors thanks all the research assistants and staff of Hospital Sirio-Libanes and HCFMUSP. RCRM and FVG are the recipients of grants FAPESP #11/08575-7, #13/20602-5 and #17/10466-8 from Brazil's government. HB is recipient of grants FAPESP and CNPQ.

DISCLOSURES

335 The authors report no conflicts of interest.ch7ng 2001

REFERENCES

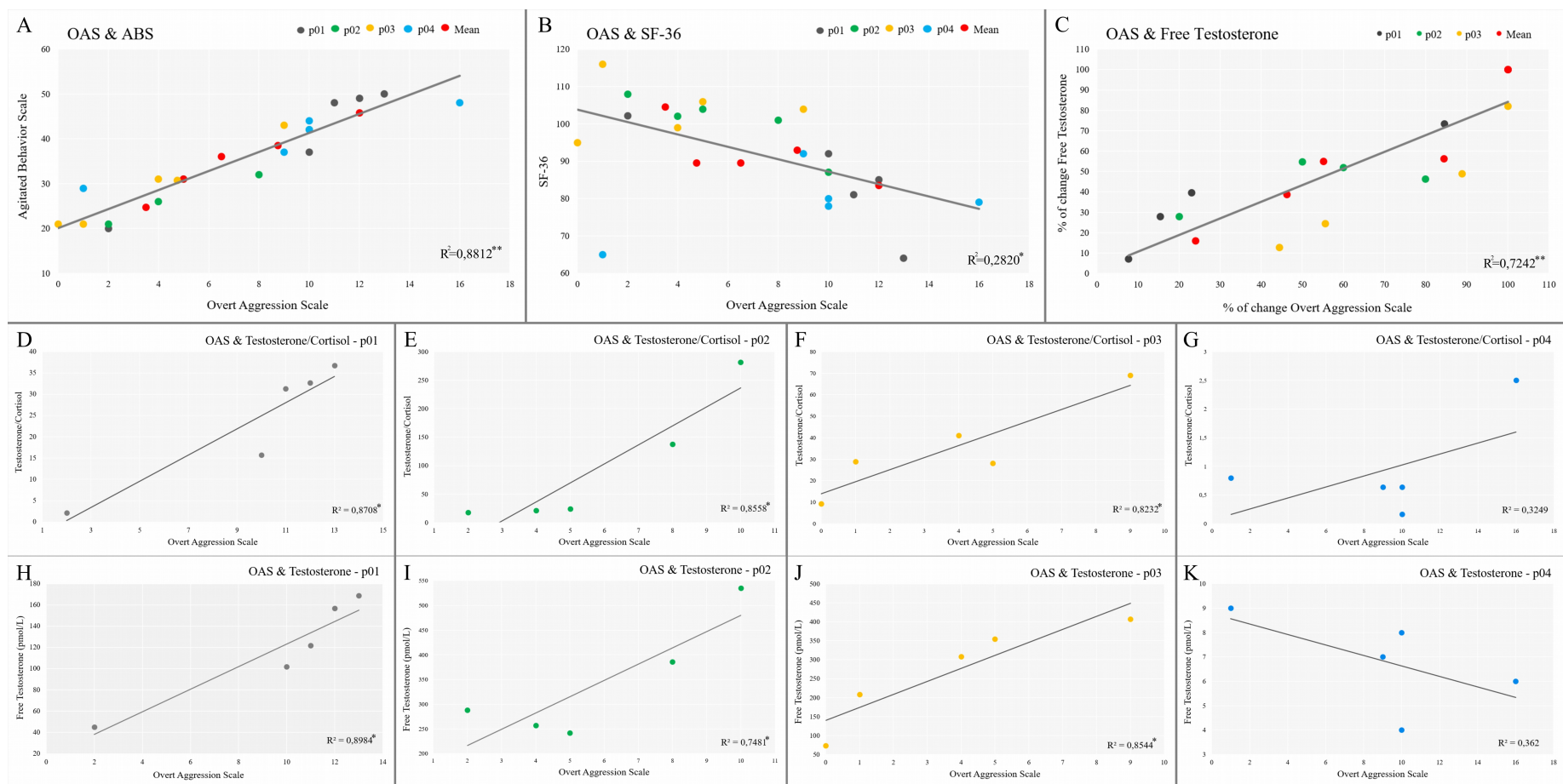
1. Brentani H de P, Silvestre C, Bordini D, et al. Autism spectrum disorders: An overview on diagnosis and treatment. *Rev Bras Psiquiatr.* 2013;35(SUPPL. 1):62-72. doi:10.1590/1516-4446-2013-S104
- 340 2. Kanne SM, Mazurek MO. Aggression in children and adolescents with ASD: Prevalence and risk factors. *J Autism Dev Disord.* 2011;41(7):926-937. doi:10.1007/s10803-010-1118-4
3. Sturm V, Fricke O, Bührle CP, et al. DBS in the basolateral amygdala improves symptoms of autism and related self-injurious behavior: a case report and hypothesis on the pathogenesis of the disorder. *Front Hum Neurosci.* 2012;6:341. doi:10.3389/fnhum.2012.00341
- 345 4. Fountas KN, Smith JR, Lee GP. Bilateral stereotactic amygdalotomy for self-mutilation disorder: Case report and review of the literature. *Stereotact Funct Neurosurg.* 2007;85(2-3):121-128. doi:10.1159/000098527
5. Comai S, Tau M, Pavlovic Z, Gobbi G. The psychopharmacology of aggressive behavior: A translational approach: Part 2: Clinical studies using atypical antipsychotics, anticonvulsants, and lithium. *J Clin Psychopharmacol.* 2012;32(2):237-260. doi:10.1097/JCP.0b013e31824929d6
- 350 6. Morissette DA, Stahl SM. Treating the violent patient with psychosis or impulsivity utilizing antipsychotic polypharmacy and high-dose monotherapy. *CNS Spectr.* 2013;19(5):439-448. doi:10.1017/S1092852914000388
- 355 7. Adler BA, Wink LK, Early M, et al. Drug-refractory aggression, self-injurious behavior, and severe tantrums in autism spectrum disorders: A chart review study. *Autism.* 2015;19(1):102-106. doi:10.1177/1362361314524641

8. Blair R. The Neurobiology of Impulsive Aggression. *J Child Adolesc Psychopharmacol*. 2016;26(1):4-9.
- 360 9. Narabayashi H, Uno M. Long range results of stereotaxic amygdalotomy for behavior disorders. *Confin Neurol*. 1966;27(1):168-171. doi:10.1159/000103950
10. Small IF, Heimburger RF, Small JG, Milstein V, Moore DF. Follow-up of stereotaxic amygdalotomy for seizure and behavior disorders. *Biol Psychiatry*. 1977;12(3):401-411.
- 365 11. Balasubramaniam V, Ramamurthi B. Stereotaxic amygdalotomy in behavior disorders. *Confin Neurol*. 1970;32(2):367-373. doi:10.1159/000103439
12. Kluver H, Bucy PC. Preliminary analysis of functions of the temporal lobes in monkeys. *Arch Neurol Psychiatry*. 1939;42(6):979-1000.
13. Rosvold HE, Mirsky AF, Pribram KH. Influence of amygdalectomy on social behavior in monkeys. *J Comp Physiol Psychol*. 1954;47(3):173-178. doi:10.1037/h0058870
- 370 14. Saxbe D, Lyden H, Gimbel SI, et al. Longitudinal Associations Between Family Aggression, Externalizing Behavior, and the Structure and Function of the Amygdala. *J Res Adolesc*. 2018;28(1):134-149. doi:10.1111/jora.12349
15. Heesink L, Gladwin TE, Vink M, van Honk J, Kleber R, Geuze E. Neural activity during the viewing of emotional pictures in veterans with pathological anger and aggression. *Eur Psychiatry*. 2018;47:1-8. doi:10.1016/j.eurpsy.2017.09.002
- 375 16. Varkeyisser T, Gladwin TE, Heesink L, van Honk J, Geuze E. Resting-state functional connectivity in combat veterans suffering from impulsive aggression. *Soc Cogn Affect Neurosci*. 2017;12(12):1881-1889. doi:10.1093/scan/nsx113

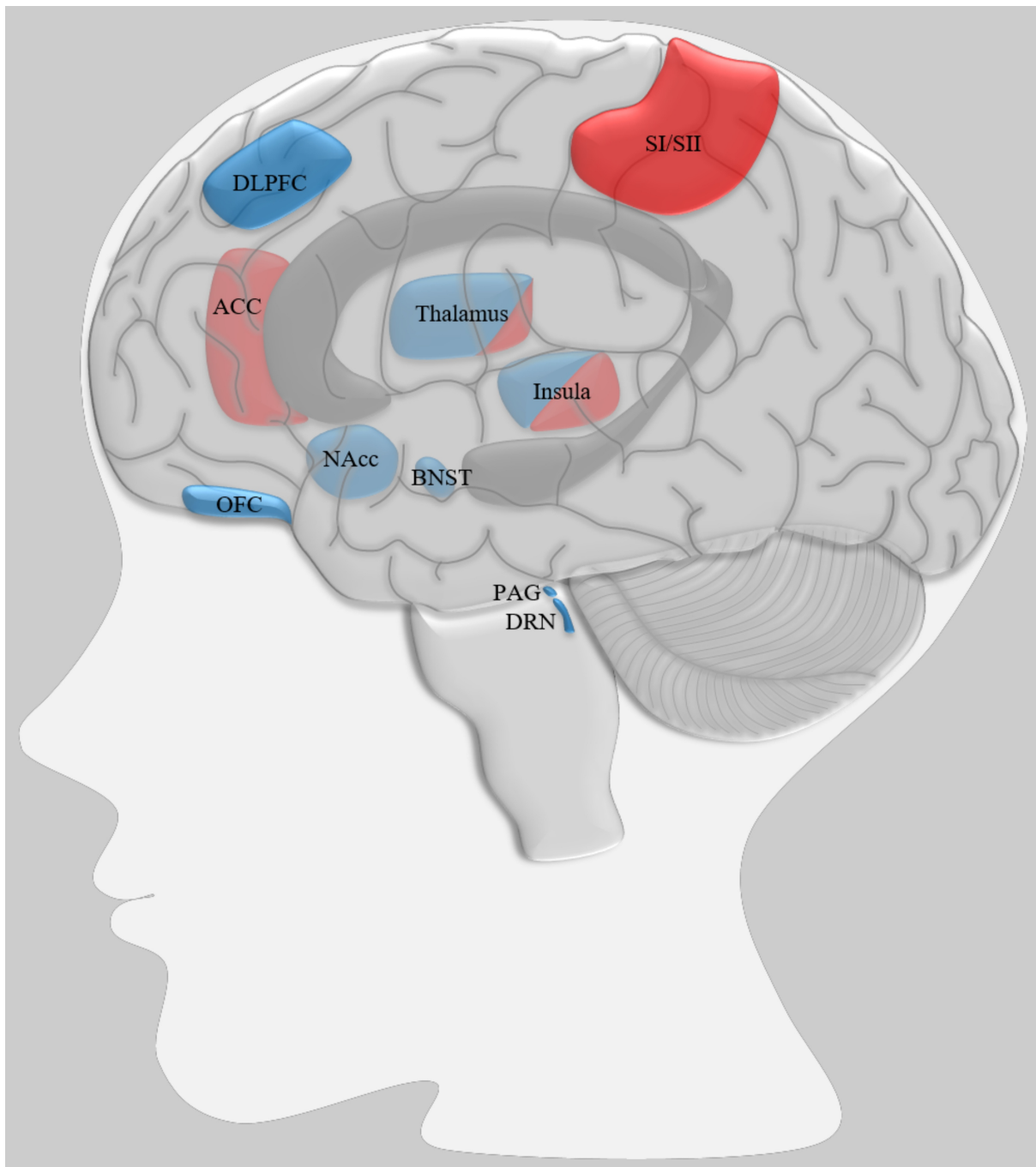
- 380 17. Kiehl KA, Smith AM, Hare RD, et al. Limbic abnormalities in affective processing by
criminal psychopaths as revealed by functional magnetic resonance imaging. *Biol Psychiatry*.
2001;50(9):677-684. doi:10.1016/S0006-3223(01)01222-7
- 385 18. Glenn AL, Raine A, Schug RA. The neural correlates of moral decision-making in
psychopathy. *Mol Psychiatry*. 2009;14(1):5-6. doi:10.1038/mp.2008.104
19. Gouveia FV, Hamani C, Fonoff ET, et al. Amygdala and Hypothalamus: Historical Overview
With Focus on Aggression. *Neurosurgery*. January 2019. doi:10.1093/neuros/hyy635
20. Zhang S, Zhou P, Jiang S, Li P, Wang W. Bilateral anterior capsulotomy and amygdalotomy
for mental retardation with psychiatric symptoms and aggression. *Med (United States)*.
2017;96(1):10-13. doi:10.1097/MD.0000000000005840
- 390 21. Brabec J, Rulseh A, Hoyt B, et al. Volumetry of the human amygdala - An anatomical study.
Psychiatry Res - Neuroimaging. 2010;182(1):67-72. doi:10.1016/j.pscychresns.2009.11.005
22. Montoya ER, Terburg D, Bos PA, van Honk J. Testosterone, cortisol, and serotonin as key
regulators of social aggression: A review and theoretical perspective. *Motiv Emot*.
2012;36(1):65-73. doi:10.1007/s11031-011-9264-3
- 395 23. Takahashi A, Miczek KA. Neurogenetics of Aggressive Behavior: Studies in Rodents. In:
Brain Imaging in Behavioral Neuroscience. ; 2013:3-44. doi:10.1007/7854_2013_263
24. Bingel U, Tracey I. Imaging CNS Modulation of Pain in Humans. *Physiology*.
2008;23(6):371-380. doi:10.1152/physiol.00024.2008
25. Chung MK, Worsley KJ, Paus T, et al. A unified statistical approach to deformation-based
morphometry. *Neuroimage*. 2001;14(3):595-606. doi:10.1006/nimg.2001.0862
- 400 26. Beaulieu C. The basis of anisotropic water diffusion in the nervous system - A technical
review. *NMR Biomed*. 2002;15(7-8):435-455. doi:10.1002/nbm.782

27. Seno MDJ, Assis D V, Gouveia F, et al. The critical role of amygdala subnuclei in nociceptive and depressive-like behaviors in peripheral neuropathy. *Sci Rep.* 2018;8(1):1-13. doi:10.1038/s41598-018-31962-w
- 405 28. Koenig J, Rinnewitz L, Warth M, et al. Psychobiological response to pain in female adolescents with nonsuicidal self-injury. *J Psychiatry Neurosci.* 2017;42(3):189-199. doi:10.1503/jpn.160074
29. Hong W, Kim D-W, Anderson DJ. Antagonistic Control of Social versus Repetitive Self-Grooming Behaviors by Separable Amygdala Neuronal Subsets. *Cell.* 2014;158(6):1348-410 1361. doi:10.1016/j.cell.2014.07.049
30. Carreño Gutiérrez H, O’Leary A, Freudenberg F, et al. Nitric oxide interacts with monoamine oxidase to modulate aggression and anxiety-like behaviour. *Eur Neuropsychopharmacol.* September 2017. doi:10.1016/j.euroneuro.2017.09.004
- 415 31. Miczek KA, Haney M. Psychomotor stimulant effects of d-amphetamine, MDMA and PCP: aggressive and schedule-controlled behavior in mice. *Psychopharmacology (Berl).* 1994;115(3):358-365. doi:10.1007/BF02245077
32. Dudas B. *The Human Hypothalamus Anatomy, Functions and Disorders.* Nova Science Publishers; 2012.
- 420 33. Tustison NJ, Cook PA, Klein A, et al. Large-scale evaluation of ANTs and FreeSurfer cortical thickness measurements. *Neuroimage.* 2014;99:166-179. doi:10.1016/j.neuroimage.2014.05.044
34. Lerch JP, Gazdzinski L, Germann J, Sled JG, Henkelman RM, Nieman BJ. Wanted dead or alive? The tradeoff between in-vivo versus ex-vivo MR brain imaging in the mouse. *Front Neuroinform.* 2012;6(March):1-9. doi:10.3389/fninf.2012.00006

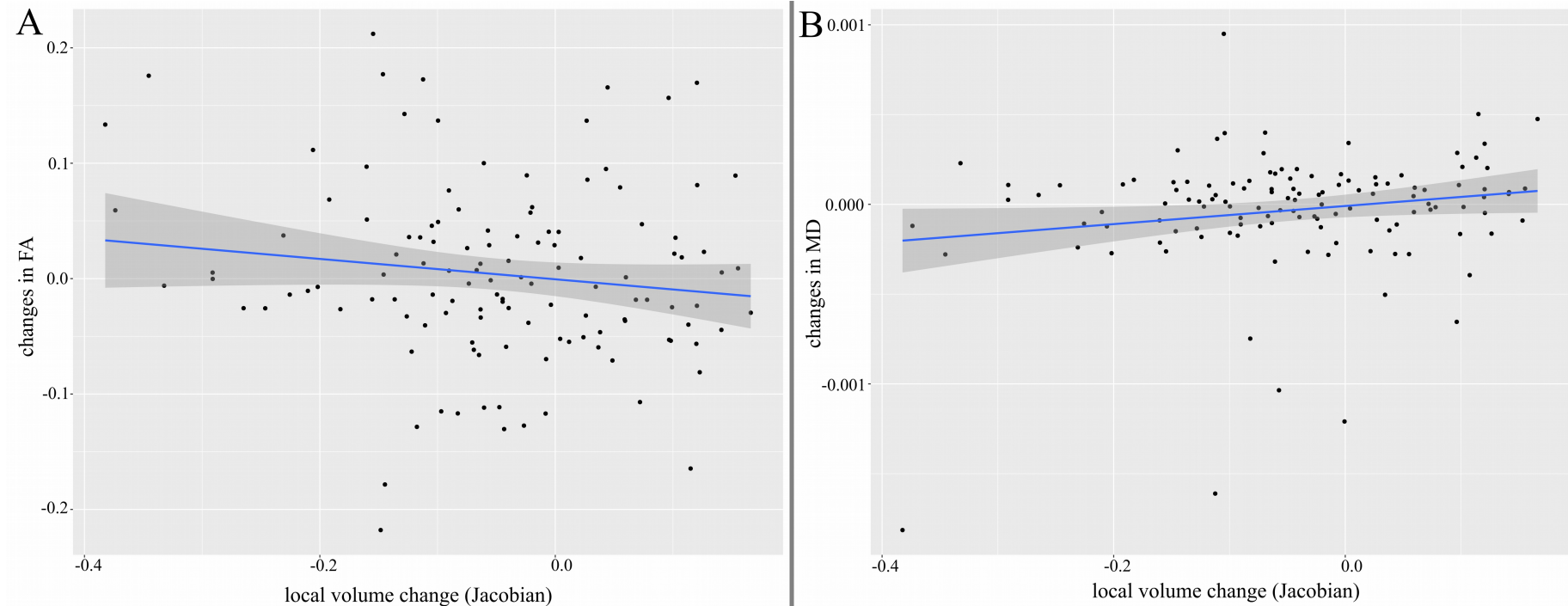
- 425 35. Smith RE, Tournier JD, Calamante F, Connelly A. SIFT: Spherical-deconvolution informed
filtering of tractograms. *Neuroimage*. 2013;67:298-312.
doi:10.1016/j.neuroimage.2012.11.049
36. Andersson JLR, Sotiroopoulos SN. An integrated approach to correction for off-resonance
effects and subject movement in diffusion MR imaging. *Neuroimage*. 2016;125:1063-1078.
430 doi:10.1016/j.neuroimage.2015.10.019
37. Veraart J, Novikov DS, Christiaens D, Ades-aron B, Sijbers J, Fieremans E. Denoising of
diffusion MRI using random matrix theory. *Neuroimage*. 2016;15(142):394-406.
doi:10.1016/j.neuroimage.2016.08.016.Denoising
38. Hawrylycz MJ, Lein ES, Guillozet-Bongaarts AL, et al. An anatomically comprehensive atlas
435 of the adult human brain transcriptome. *Nature*. 2012;489(7416):391-399.
doi:10.1038/nature11405
39. Eden E, Navon R, Steinfeld I, Lipson D, Yakhini Z. GOrilla: A tool for discovery and
visualization of enriched GO terms in ranked gene lists. *BMC Bioinformatics*. 2009;10:1-7.
doi:10.1186/1471-2105-10-48
- 440 40. Subramanian A, Tamayo P, Mootha VK, et al. Gene set enrichment analysis: A knowledge-
based approach for interpreting genome-wide expression profiles. *Proc Natl Acad Sci*.
2005;102(43):15545-15550. doi:10.1073/pnas.0506580102



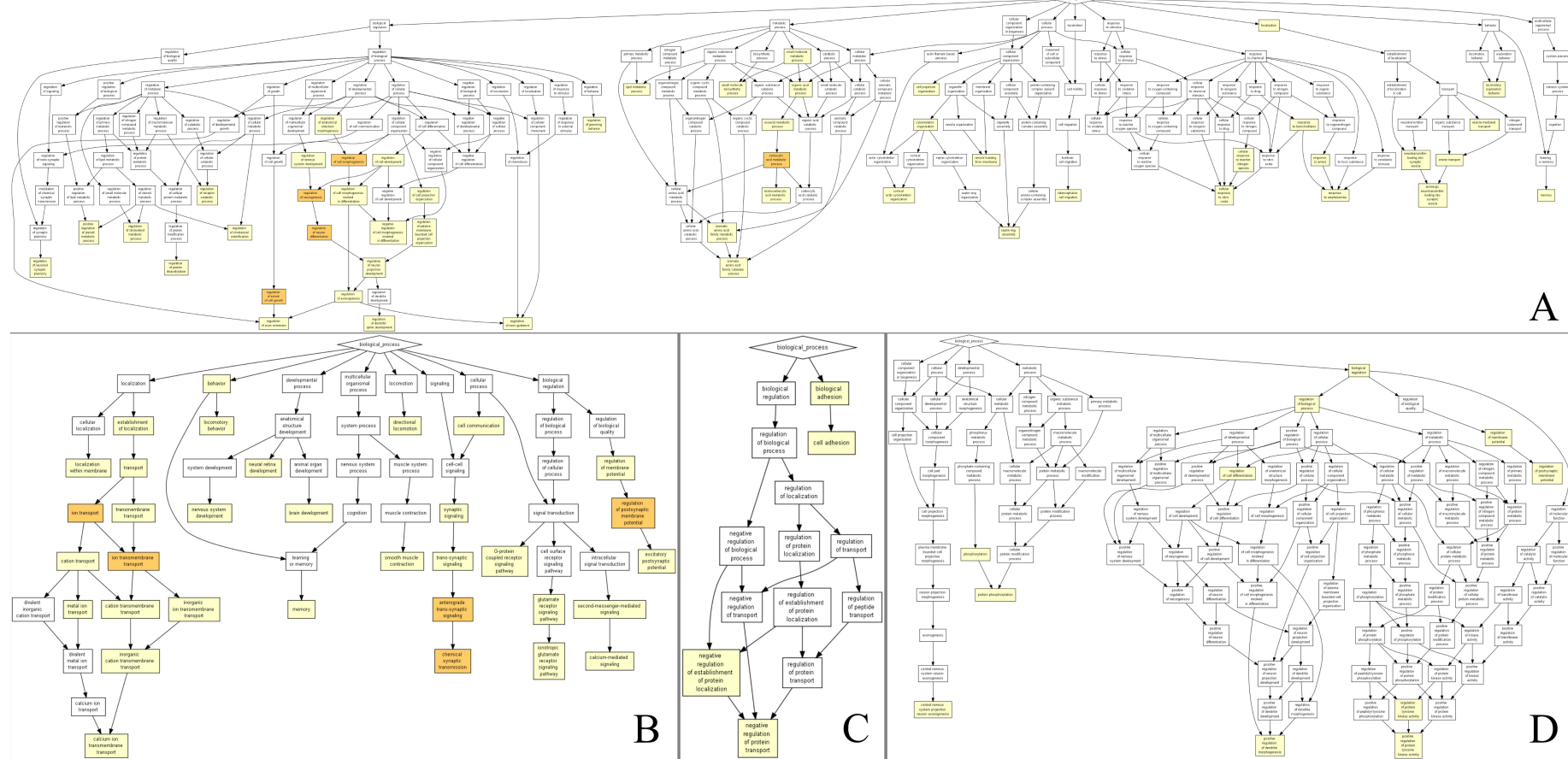
Supplementary Figure 1. Hormonal and behavior correlations. A. Aggressive Behavior (Overt Aggression Scale - OAS) and Agitation (Agitated Behavior Scale - ABS). B. Aggressive Behavior (OAS) and Quality of life (SF-36). C. % of change in aggressive behavior (OAS) and % of change in Free Testosterone. D-G. Individual analysis of aggressive behavior and free testosterone (p01-p04). H-K. Individual analysis of aggressive behavior and testosterone/cortisol ratio (p01-p04). * $p<0.05$; ** $p<0.01$



Supplementary Figure 2. Illustration representing the main changes in areas related to cluster 1 aggressive behavior (blue, decreases in volume) and cluster 2 somatosensation (red, increases in volume). Abbreviations: ACC: anterior cingulate cortex; BNST: bed nucleus of stria terminalis; DLPFC: dorsolateral prefrontal cortex; DRN: dorsal raphe nucleus; NAcc: nucleus accumbens; OFC: orbitofrontal cortex; PAG: periaqueductal gray; SI/SII: somatosensory cortex.



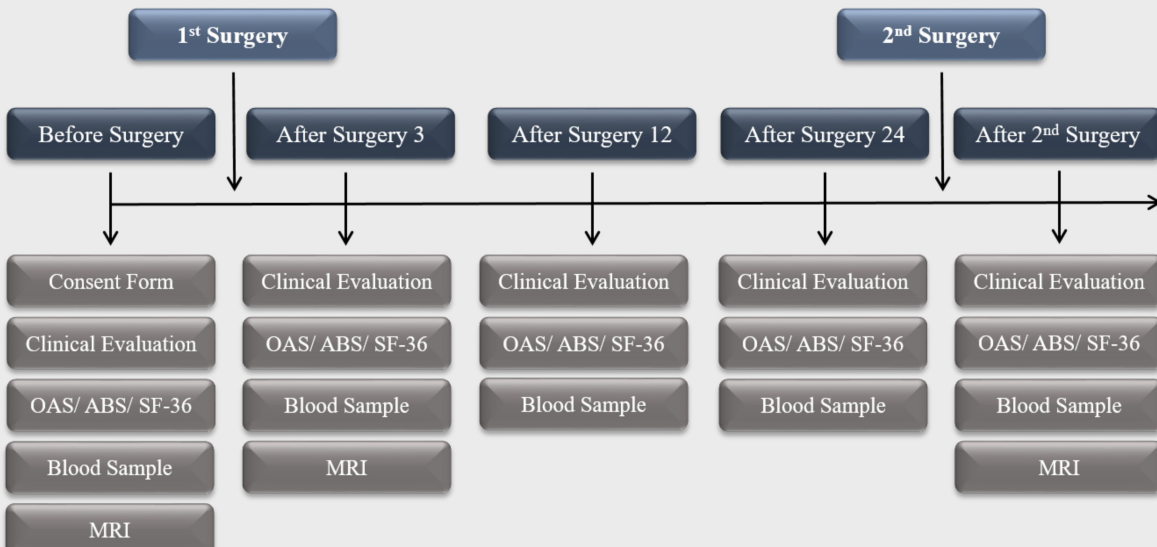
Supplementary Figure 3: Correlation between DBM Jacobians, FA and MD maps for all peaks. A. Correlations between local volume change in Jacobian and FA map. B. Correlations between local volume change in Jacobian and MD map.



Supplementary Figure 4. Results of gene enrichment analysis using the GOrilla gene ontology tool. A. Highly expressed genes in areas of volumes decrease (DBM). B. Low expressed genes in areas of volumes decrease (DBM). C. Low expressed genes in areas of volumes increase (DBM). D. Highly expressed genes in areas of volumes increase (DBM).

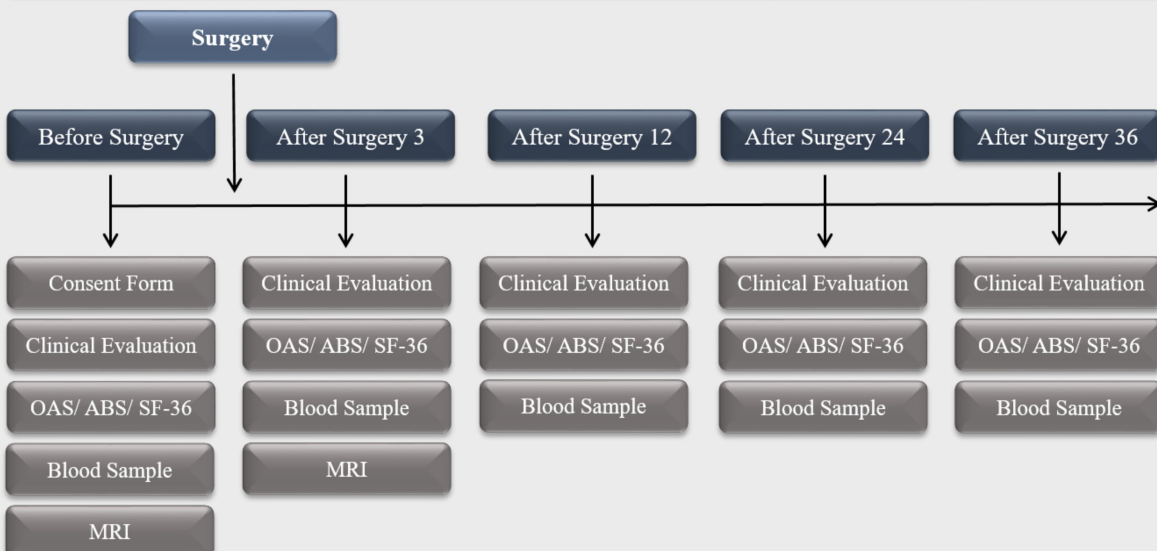
A

Study Design – p01; p02; p04



B

Study Design – p03



Supplementary Figure 5. Study design. A. Study design for patients p01, p02 and p04. B. Study design for patient p03. Abbreviations: After surgery 3, 12, 24 and 36: 3, 12, 24 and 36 months after surgery, respectively; OAS: Overt Aggression Scale; ABS: Agitated Behavior Scale; MRI: Magnetic Resonance Imaging.

Supplementary Table 1. Data from laboratorial blood test.

	Patient p01					Patient p02					Patient p03					Patient p04				
	1 st	2 nd	3 rd	4 th	5 th	1 st	2 nd	3 rd	4 th	5 th	1 st	2 nd	3 rd	4 th	5 th	1 st	2 nd	3 rd	4 th	5 th
TSH (mIU/L)	1.83	1.58	2.24	2.16	2.76	0.89	0.91	1.11	0.94	1.74	1.75	0.78	1.39	1.49	2.32	2.56	1.56	1.99	3.66	1.13
Free T4 (ng/dL)	1.58	1.18	1.01	1.25	01.09	1.44	1.48	1.49	1.48	1.72	1.16	0.94	0.75	0.91	0.84	1.31	01.04	1.33	0.99	1.16
T3 (mg/dL)	0.13	0.10	0.10	0.10	0.12	110	110	120	120	0.15	0.81	0.81	0.72	0.69	0.81	0.13	0.07	0.09	0.10	0.09
Cortisol (mg/dL)	4.60	3.90	6.50	4.80	21.50	1.90	10.10	12.20	2.80	16.5	5.90	7.90	7.50	12.60	7.20	2.40	12.50	11.30	24.16	11.00
LH (IU/L)	1.70	6.00	1.40	1.30	2.30	3.40	0.80	9.50	6.30	8.4	1.80	2.00	7.00	10.40	5.60	6.30	0.30	18.80	9.98	14.50
FSH (IU/L)	1.30	2.40	0.60	0.90	0.60	5.90	3.60	7.40	6.80	3.8	2.00	1.70	2.90	3.00	3.10	5.10	2.10	6.20	6.61	5.80
Estradiol (pg/mL)	17.00	19.00	15.00	21.10	24.80	55.00	23.00	24.10	44.30	30.2	30.00	18.00	15.00	15.00	29.50	27.00	16.00	18.50	26.79	15.00
Prolactin (mg/dL)	0.57	0.69	0.69	0.85	0.74	3.20	4.30	5.30	5.80	4.2	60.10	19.20	7.50	8.40	11.60	95.40	45.30	107.9	100.2	64.10
Progesterone (ng/mL)	0.30	0.30	0.50	0.40	0.50	0.30	0.30	0.40	0.40	0.6	0.30	0.40	0.30	0.30	0.30	0.30	0.90	0.30	0.10	0.30
Total Testosterone (ng/mL)	336	198	115	350	115	412	310	281	428	279	409	97.00	528	634	359	18.00	22.00	29.00	53.73	22.00
Free Testosterone (pmol/L)	169	122	102	157	45.00	535	242	257	386	288	407	73.00	308	355	208	6.00	8.00	9.00	0.40	7.00
SHBG (nmol/L)	57.00	45.00	50.20	62.60	76.80	17.00	20.00	26.10	21.00	13.6	26.00	26.00	44.70	52.30	48.30	81.00	78.00	93.80	113	91.90
Urea (mg/dL)	31.00	27.00	39.00	33.00	31.00	35.00	19.00	33.00	25.00	28.00	22.00	20.00	20.00	19.00	13.00	28.00	28.00	18.00	31.00	20.00
Creatinine (mg/dL)	0.76	0.75	0.97	0.86	0.87	0.86	0.80	0.90	0.78	0.84	0.86	0.81	0.92	0.83	0.70	0.84	0.72	0.56	0.65	0.61
Sodium (mEq/L)	140	144	141	138	141	140	145	138	145	144	137	130	131	139	129	142	144	142	142	140
Potassium (mEq/L)	4.40	4.10	4.70	3.70	4.20	3.90	4.70	4.40	4.30	4.20	4.00	4.10	4.50	4.50	4.70	4.00	4.10	4.10	3.80	4.00
AST (U/L)	19.00	21.00	23.00	11.00	16.00	16.00	16.00	12.00	16.00	14.00	25.00	21.00	17.00	19.00	21.00	25.00	27.00	29.00	32.00	29.00
ALT (U/L)	23.00	23.00	23.00	17.00	15.00	20.00	15.00	11.00	14.00	17.00	26.00	23.00	17.00	17.00	21.00	40.00	37.00	41.00	40.00	39.00
Total Bilirubin (mg/dL)	0.16	0.38	0.54	0.16	0.29	0.28	0.56	0.32	0.42	0.36	0.25	0.32	0.28	0.42	0.36	0.33	0.45	0.47	0.37	0.39
Total Cholesterol (mg/dL)	221	221	181	180	227	159	157	142	153	149	256	245	238	261	212	149	137	152	148	163
Triglycerides (mg/dL)	218	103	116	137	208	164	131	138	146	195	183	245	280	373	176	131	131	132	131	130
HDL (mg/dL)	39.00	52.00	51.00	60.00	46.00	35.00	28.00	32.00	40.00	42.00	67.00	48.00	56.00	46.00	65.00	26.00	32.00	24.00	26.00	36.00
LDL (mg/dL)	138	115	107	93.00	139	96.00	75.00	85.00	76.00	70.00	110	136	123	151	112	73.00	75.00	82.00	77.00	79.00
C-reactive protein (mg/L)	2.60	3.20	12.60	0.90	1.30	11.20	7.60	3.10	9.60	6.30	1.00	2.30	1.50	1.70	2.00	1.60	2.30	1.80	2.20	3.00
Platelets (th/mm3)	301	292	327	212	267	165	135	234	184	196	214	173	183	202	166	96.00	89.00	92.00	102	83.00
MPV (fL)	9.70	9.70	9.90	9.50	9.00	11.80	11.30	12.30	11.60	11.80	9.70	10.00	9.40	9.00	9.10	11.90	11.80	11.90	12.30	11.90
Erythrocytes (mil/mm3)	5.49	4.94	5.36	4.92	4.93	5.49	5.16	5.75	5.58	5.48	4.66	4.46	4.47	4.42	4.37	4.38	3.93	4.38	4.28	4.65
Hemoglobin (g/dL)	16.20	14.70	16.20	15.50	15.70	13.60	13.00	12.70	12.10	14.90	14.60	14.10	14.00	14.10	13.70	14.40	12.60	14.00	13.80	14.90
Hematocrit (%)	46.20	42.00	46.30	44.90	44.30	41.40	39.90	40.70	39.00	44.70	41.6	39.90	40.30	38.20	38.70	42.50	36.80	40.20	40.00	42.40
MCV (fL)	84.20	85.00	86.40	91.30	89.90	75.40	77.30	70.80	69.90	81.60	89.30	89.50	90.20	86.40	88.60	97.00	93.60	91.80	93.50	91.20
MCH (pg)	29.50	29.80	30.20	31.50	31.80	24.80	25.20	22.10	21.70	27.20	31.30	31.60	31.30	31.90	31.40	32.90	32.10	32.00	32.20	32.00
MCHC (g/dL)	35.10	35.00	35.00	34.50	35.40	32.90	32.60	31.20	31.00	33.30	35.10	35.30	34.70	36.90	35.40	33.90	34.20	34.80	34.50	35.10
RDW-CV (%)	12.80	12.80	12.30	12.90	12.60	19.80	19.30	20.00	19.10	16.50	12.30	12.20	12.10	12.00	12.30	12.50	12.20	12.40	12.10	12.10
RDW-SD (fL)	38.80	39.00	38.60	42.20	41.30	51.70	53.10	50.00	48.70	48.70	39.50	39.00	39.30	37.00	39.80	43.60	40.90	42.00	40.90	39.50
Leukocytes (th/mm3)	4.77	6.19	4.99	9.48	5.95	09.01	5.46	7.47	6.86	6.58	4.62	6.18	4.49	4.20	4.30	3.76	3.81	2.67	4.60	6.61
Neutrophils (%)	42.10	85.40	37.10	39.70	30.20	75.30	63.60	5.47	71.90	65.80	42.10	37.00	38.30	34.20	30.20	49.00	50.70	48.00	45.00	84.40
Eosinophils (%)	4.60	0.20	5.20	0.30	4.50	1.90	2.90	0.15	2.90	1.70	0.40	0.50	0.20	0.70	0.50	1.60	2.60	0.70	1.30	0.30
Basophils (%)	0.20	0.00	0.20	0.10	0.20	0.60	0.50	0.05	0.60	0.60	0.40	0.20	0.40	0.50	0.00	0.00	0.30	0.40	0.20	0.00
Lymphocyte (%)	43.00	11.80	42.70	47.50	50.80	12.80	22.70	1.19	16.30	22.30	43.50	51.90	44.80	49.80	56.70	42.80	35.40	43.80	42.00	12.90
Monocytes (%)	10.10	2.60	14.80	12.40	14.30	9.40	10.30	0.61	8.30	9.60	13.60	10.40	16.30	14.80	12.60	6.60	11.00	7.10	11.50	2.40

Abbreviations: 1st: Before surgery; 2nd: 3 months after surgery; 3rd: 12 months after surgery; 4th: 24 months after surgery; 5th: 36 months after surgery for p03 and after second surgery for p01, p02, p04; TSH: Thyroid-Stimulating Hormone; Free T4: Free Thyroxine; T3: Triiodothyronine; LH: Luteinizing Hormone; FSH: Follicle-Stimulating Hormone; SHBG: Sex Hormone Binding Globulin; AST: Aspartate Aminotransferase; ALT: Alanine Aminotransferase; HDL: High-Density Lipoprotein; LDL: Low-Density Lipoprotein; MPV: Mean Platelet Volume; MCV: Mean Corpuscular Volume; MCH: Mean Cell Hemoglobin; MCHC: Mean Cell Hemoglobin Concentration; RDW-CV: Red Cell Distribution Width – Cell Volume; RDW-SD: Red Cell Distribution Width – Standard Deviation.